Universität Augsburg

Institut für Mathematik

Ronald H.W. Hoppe and Joachim Schöberl

Convergence of Adaptive Edge Element Methods for the 3D Eddy Currents Equations

Preprint Nr. 038/2007 — 26. Oktober 2007

Institut für Mathematik, Universitätsstraße, D-86 135 Augsburg http://www.math.uni-augsburg.de/

Impressum:

Herausgeber:

Institut für Mathematik
Universität Augsburg
86135 Augsburg
http://www.math.uni-augsburg.de/forschung/preprint/

ViSdP:

Ronald H.W. Hoppe
Institut für Mathematik
Universität Augsburg
86135 Augsburg

CONVERGENCE OF ADAPTIVE EDGE ELEMENT METHODS FOR THE 3D EDDY CURRENTS EQUATIONS

R.H.W. HOPPE * AND J. SCHÖBERL †

Abstract. We consider an Adaptive Edge Finite Element Method (AEFEM) for the 3D eddy currents equations with variable coefficients using a residual-type a posteriori error estimator. Both the components of the estimator and certain oscillation terms, due to the occurrence of the variable coefficients, have to be controlled properly within the adaptive loop which is taken care of by appropriate bulk criteria. Convergence of the AEFEM in terms of reductions of the energy norm of the discretization error and of the oscillations is shown. Numerical results are given to illustrate the performance of the AEFEM.

Key words. adaptive edge elements, 3D eddy currents equations, convergence analysis, error and oscillation reduction, residual type a posteriori error estimates

AMS subject classifications. 65F10, 65N30

1. Introduction.

The numerical solution of the 3D Maxwell equations is one of the most important issues in computational electromagnetics. During the past decade, significant progress has been made with regard to the development of efficient Finite Element Methods (FEM) for interior domain problems, Boundary Element Methods (BEM) for exterior domain problems, and BEM-FEM approaches for coupled exterior/interior domain problems. We refer to the survey article [21], the recent monograph [24], and the proceedings [14] for an overview of the state-of-the-art and an extensive bibliography.

We assume Ω to be a bounded domain in $\mathbb{R}^3$ with polyhedral boundary $\Gamma = \partial\Omega$. We adopt standard notation from Lebesgue and Sobolev space theory. In particular, $L^2(\Omega)$ (resp. $\mathbf{L^2}(\Omega)$) stands for the Hilbert space of square integrable functions (resp. vector fields) on Ω with norm $\|\cdot\|_{0,\Omega}$, whereas $H^m(\Omega), m \in \mathbb{N}$ (resp, $\mathbf{H^m}(\Omega)$) refer to the Sobolev spaces of functions (resp. vector fields) on Ω.

We define $\mathbf{H}(\mathbf{curl};\boldsymbol{\Omega}) := \{\mathbf{q} \in \mathbf{L^2}(\boldsymbol{\Omega}) | \mathbf{curl}\ \mathbf{q} \in \mathbf{L^2}(\boldsymbol{\Omega})\}$ as the Hilbert space equipped

*Institut fur Mathematik, Universitat Augsburg, D-86159, Augsburg, Germany, and Department of Mathematics, University of Houston, Houston, TX 77204-3008, USA (hoppe@math.uni-augsburg.de,rohop@math.uh.edu)

†Dept. for Mathematics CCES (Center for Computational Engineering Science), RWTH Aachen, D-52074 Aachen, Germany (joachim.schoeberl@rwth-aachen.de)

with with the graph norm $\|\mathbf{q}\|_{curl;\Omega} := (\|\mathbf{q}\|_{0,\Omega}^2 + \|\mathbf{curl}\ \mathbf{q}\|_{0,\Omega}^2)^{1/2}$. We further refer to

$$\boldsymbol{\gamma}_\Gamma(\mathbf{q}) := \mathbf{q} \wedge \mathbf{n}_\Gamma \in \mathbf{H}^{-1/2}(\mathrm{div}_F; \Gamma) \tag{1.1}$$

as the tangential trace and to

$$\boldsymbol{\pi}_\Gamma(\mathbf{q}) := \mathbf{n}_\gamma \wedge (\mathbf{q} \wedge \mathbf{n}_\gamma) \in \mathbf{H}^{-1/2}(\mathrm{curl}_F; \Gamma) \tag{1.2}$$

as the tangential components trace of $\mathbf{q} \in \mathbf{H}(\mathbf{curl}; \Omega)$, where $\mathbf{n}_\Gamma$ denotes the outward unit normal on Γ and $\mathrm{div}_\Gamma, \mathrm{curl}_\Gamma$ stand for the surfacic divergence and surfacic rotational, respectively (for a proper definition of these mappings and the associated trace spaces cf., e.g., [11, 12, 13]).

We further refer to $\mathbf{H}(\mathrm{div}; \Omega) := \{\mathbf{q} \in \mathbf{L}^2(\Omega) | \mathrm{div}(\mathbf{q}) \in L^2(\Omega)\}$ as the Hilbert space with the graph norm $\|\mathbf{q}\|_{div,\Omega} := \left(\|\mathbf{q}\|_{0,\Omega}^2 + \|\mathrm{div}(\mathbf{q})\|_{0,\Omega}^2\right)^{1/2}$ and denote by $\boldsymbol{\nu}_\Gamma(\mathbf{q}) := \mathbf{n}_\Gamma \cdot \mathbf{q} \in H^{-1/2}(\Gamma)$ the normal trace of $\mathbf{q} \in \mathbf{H}(\mathrm{div}; \Omega)$ on Γ. We note that for a simply connected, polyhedral subset $D \subseteq \Omega$, the spaces $\mathbf{H}(\mathbf{curl}; D)$ and $\mathbf{H}(\mathrm{div}; D)$ as well as the associated trace mappings $\boldsymbol{\gamma}_{\partial D}, \boldsymbol{\pi}_{\partial D}$ and $\boldsymbol{\nu}_{\partial D}$ are defined analogously. In particular, $\boldsymbol{\gamma}_{\partial D} : \mathbf{H}(\mathbf{curl}; D) \to \mathbf{H}^{-1/2}(\mathrm{div}_{\partial D}; \partial D), \boldsymbol{\pi}_{\partial D} : \mathbf{H}(\mathbf{curl}; D) \to \mathbf{H}^{-1/2}(\mathrm{curl}_{\partial D}; \partial D)$ and $\boldsymbol{\nu}_{\partial D} : \mathbf{H}(\mathrm{div}; \Omega) \to H^{-1/2}(\partial D)$ are surjective and continuous, linear mappings such that

$$\|\boldsymbol{\gamma}_{\partial D}(\mathbf{q})\|_{||,-1/2,\partial D} \lesssim \|\mathbf{q}\|_{curl;\Omega} \quad , \quad \mathbf{q} \in \mathbf{H}(\mathbf{curl}; D) \ , \tag{1.3}$$

$$\|\boldsymbol{\pi}_{\partial D}(\mathbf{q})\|_{\perp,-1/2,\partial D} \lesssim \|\mathbf{q}\|_{curl;\Omega} \quad , \quad \mathbf{q} \in \mathbf{H}(\mathbf{curl}; D) \ , \tag{1.4}$$

$$\|\boldsymbol{\nu}_{\partial D}(\mathbf{q})\|_{-1/2,\partial D} \lesssim \|\mathbf{q}\|_{div;\Omega} \quad , \quad \mathbf{q} \in \mathbf{H}(\mathrm{div}; D) \ , \tag{1.5}$$

where $\|\cdot\|_{||,-1/2,\partial D}, \|\cdot\|_{\perp,-1/2,\partial D}, \|\cdot\|_{-1/2,\partial D}$ refer to the norms on $\mathbf{H}^{-1/2}(\mathrm{div}_{\partial D}; \partial D)$, $\mathbf{H}^{-1/2}(\mathrm{curl}_{\partial D}; \partial D)$ and $H^{-1/2}(\partial D)$, respectively (cf., e.g., [13]).

We introduce the subspace

$$\mathbf{H_0}(\mathbf{curl}; \Omega) \ := \ \{\mathbf{q} \in \mathbf{H}(\mathbf{curl}; \Omega) \mid \boldsymbol{\pi}_\Gamma(\mathbf{q}) = \mathbf{0}\} \tag{1.6}$$

and define the bilinear form $a(\cdot,\cdot) : \mathbf{H_0}(\mathbf{curl};\Omega) \times \mathbf{H_0}(\mathbf{curl};\Omega) \to \mathbb{R}$ according to

$$a(\mathbf{j},\mathbf{q}) \;:=\; \int\limits_\Omega \big(\chi \mathbf{curl}\,\mathbf{j} \cdot \mathbf{curl}\,\mathbf{q} + \kappa \mathbf{j} \cdot \mathbf{q}\big)\; dx \quad , \quad \mathbf{j},\mathbf{q} \in \mathbf{H_0}(\mathbf{curl};\Omega) \;. \tag{1.7}$$

We assume $\chi, \kappa \in L^\infty(\Omega)$ such that $\chi \geq \chi_0$ a.e. and $\kappa \geq \kappa_0$ a.e. for some $\chi_0, \kappa_0 \in \mathbb{R}_+$. Hence, the bilinear form $a(\cdot,\cdot)$ is $\mathbf{H_0}(\mathbf{curl};\Omega)$-elliptic and defines an equivalent norm on $\mathbf{H_0}(\mathbf{curl};\Omega)$ according to

$$|||\mathbf{q}|||^2 \;:=\; a(\mathbf{q},\mathbf{q}) \quad , \quad \mathbf{q} \in \mathbf{H_0}(\mathbf{curl};\Omega) \;. \tag{1.8}$$

Moreover, we suppose that $\mathbf{f} \in \prod_{i=1}^m \mathbf{H}(\mathrm{div};\Omega_i)$ and $\chi, \kappa \in \prod_{i=1}^m W^{1,\infty}(\Omega_i)$ with regard to a partition of Ω into non overlapping subdomains $\Omega_i, 1 \leq i \leq m$. We consider the following variational problem:

Find $\mathbf{j} \in \mathbf{H_0}(\mathbf{curl};\Omega)$ such that

$$a(\mathbf{j},\mathbf{q}) \;=\; \int\limits_\Omega \mathbf{f} \cdot \mathbf{q}\; dx \quad , \quad \mathbf{q} \in \mathbf{H_0}(\mathbf{curl};\Omega) \;. \tag{1.9}$$

It is well-known that under the given assumptions (1.9) admits a unique solution.

For the edge element discretization of (1.9) we consider a shape regular simplicial triangulation $\mathcal{T}_H$ of Ω which is consistent with the partition $\overline{\Omega} = \prod\limits_{i=1}^{m} \overline{\Omega}_i$ in the sense that each $\Omega_i, 1 \leq i \leq m$, inherits a shape regular, simplicial triangulation $\mathcal{T}_H(\Omega_i)$. We refer to $\mathcal{N}_H(D), \mathcal{E}_H(D), \mathcal{F}_H(D)$, and $\mathcal{T}_H(D)$ as the sets of vertices, edges, faces, and elements of the triangulation in $D \subseteq \bar{\Omega}$. We denote by h_T (h_F) the diameter of an element $T \in \mathcal{T}_H(\Omega)$ (face $F \in \mathcal{F}_H$) and by h_E the length of an edge $E \in \mathcal{E}_H(\Omega)$. Further, we refer to $\omega_F = T_+ \cup T_-$ as the union of the triangles $T_\pm \in \mathcal{T}_H$ sharing the common face $F \in \mathcal{F}_H(\Omega)$. Throughout the sequel, for two quantities A and B we will use the notation $A \lesssim B$, if there exists a constant $\gamma > 0$, depending only on the data of the problem and on the shape regularity of the triangulations, such that $A \leq \gamma B$.

The variational equation (1.9) is discretized by the lowest order edge elements of Nédélec's first family

$$\mathbf{Nd}_1(T) \;:=\; \{\; \exists \boldsymbol{\alpha} \in \mathbb{R}^3, \exists \boldsymbol{\beta} \in \mathbb{R}^3 \;\forall \mathbf{x} = (x_1,x_2,x_3) \in T : \;\mathbf{q}(x) = \boldsymbol{\alpha} + \boldsymbol{\beta} \wedge \mathbf{x} \;\} \;.$$

The associated curl-conforming edge element space $\mathbf{Nd_1}(\Omega;\mathcal{T}_H(\Omega)) \subset \mathbf{H}(\mathbf{curl};\Omega)$ is given by

$$\mathbf{Nd}_1(\Omega;\mathcal{T}_H) \ := \ \{ \ \mathbf{q}_H \in \mathbf{H}(\mathbf{curl};\Omega) \mid \mathbf{q}_H|_T \in \mathbf{Nd}_1(T) \ , \ T \in \mathcal{T}_H \ \} \ ,$$

and we refer to $\mathbf{Nd_{1,0}}(\Omega;\mathcal{T}_H(\Omega))$ as its subspace

$$\mathbf{Nd_{1,0}}(\Omega;\mathcal{T}_H) \ := \ \{ \ \mathbf{q}_H \in \mathbf{Nd_1}(\Omega;\mathcal{T}_H) \mid \boldsymbol{\pi}_\Gamma(\mathbf{q}_H) = 0 \text{ on } \Gamma \ \} \ .$$

Then, the edge element discretization of (1.9) amounts to the computation of $\mathbf{j}_H \in \mathbf{Nd_{1,0}}(\Omega;\mathcal{T}_H)$ such that

$$a(\mathbf{j}_H, \mathbf{q}_H) \ = \ \int_\Omega \mathbf{f} \cdot \mathbf{q}_H \quad , \quad \mathbf{q}_H \in \mathbf{Nd_{1,0}}(\Omega;\mathcal{T}_H). \tag{1.10}$$

An Adaptive Finite Element Method (AFEM) consists of successive loops of the cycle

$$\text{SOLVE} \rightarrow \text{ESTIMATE} \rightarrow \text{MARK} \rightarrow \text{REFINE} \ . \tag{1.11}$$

Here, SOLVE stands for the numerical solution of the finite element discretized problem, ESTIMATE requires the a posteriori estimation of the global discretization error in some appropriate norm or with respect to a goal oriented error functional. The step MARK is devoted to the selection of elements and edges for refinement, and the final step REFINE takes care of the technical realization of the refinement process.

The development, analysis and implementation of efficient and reliable a posteriori error estimators has been the subject of intensive research in the past two decades and has actually reached some level of maturity (see, e.g., the monographs [1, 4, 5, 19, 27, 32] and the references therein). On the other hand, a rigorous convergence analysis of (1.11) relying on appropriate error reduction properties has so far only been done for conforming AFEMs [18, 25, 23] and, very recently, by the first two authors for mixed and nonconforming finite element methods in [15, 16]. Optimal convergence rates for conforming AFEMs have been obtained in [9] and [31].

In this paper, we will be concerned with a convergence analysis of adaptive edge element approximations of the 3D eddy currents equations in the stationary case. We note that efficient and reliable a posteriori error estimators have been developed and analyzed in [6, 7, 8, 22, 30]. On the other hand, as far as a convergence analysis by means of a guaranteed error reduction within the adaptive loop is concerned, so far only the 2D equations have been considered assuming constant coefficients [15]. Here, we will address the more realistic 3D scenario with variable coefficients which gives rise to additional oscillations which can be treated following similar arguments as in the convergence analysis of AFEMs for general linear second order elliptic PDEs [23]. The paper is organized as follows. Section 2 describes the adaptive loop including the reliability of the error estimator and states the main convergence result. Section 3 is concerned with an error reduction result by means of the discrete local efficiency of the estimator, whereas Section 4 establishes oscillation reduction. Section 5 contains the proof of the main convergence result which follows from the error and the oscillation reduction properties. Finally, Section 6 contains a documentation of numerical results illustrating the performance of the adaptive edge element method.

2. Adaptive loop and main convergence result. The step SOLVE in the adaptive loop (1.11) requires the numerical solution of the edge element discretized problem (1.10) for which efficient multilevel techniques have been derived in [3, 20, 28] (cf. also [6, 21, 24]).

For the following step ESTIMATE, we will provide a residual-type a posteriori error estimator similar to those considered in [7] and [30]. For this purpose, we consider the element residuals

$$R_T^{(1)}(\mathbf{j_H}) := \mathbf{curl}(\chi \mathbf{curl}(\mathbf{j_H})) \ + \ \kappa \mathbf{j_H} \ - \ \mathbf{f} \quad , \quad T \in \mathcal{T}_H \ , \tag{2.1}$$

$$R_T^{(2)}(\mathbf{j_H}) := \mathrm{div}(\kappa \mathbf{j_H}) \ - \ \mathrm{div}(\mathbf{f}) \quad , \quad T \in \mathcal{T}_H \ , \tag{2.2}$$

and the face residuals associated with interior faces

$$R_F^{(1)}(\mathbf{j_H}) := [\chi \mathbf{curl}(\mathbf{j_H}) \wedge \mathbf{n}_F]_F \quad , \quad F \in \mathcal{F}_H(\Omega) \ , \tag{2.3}$$

$$R_F^{(2)}(\mathbf{j_H}) := [\mathbf{n}_F \cdot \kappa \mathbf{j_H} - \mathbf{f}]_F \quad , \quad F \in \mathcal{F}_H(\Omega) \ , \tag{2.4}$$

where $[\cdot]_F$ denotes the jump across F.

Since we only want to select faces for refinement in the bulk criterion, for an interior face $F = T_+ \cap T_-, T_\pm \in \mathcal{T}_H$, we define $\eta_F^{(1)}$ as a weighted sum of the $\mathbf{L^2}$-norms of the element residuals $R_{T_\pm}^{(\nu)}(\mathbf{j_H}), 1 \le \nu \le 2$, according to

$$(\eta_F^{(1)})^2 := \frac{h_{T_+}^2}{m_+}\Big(\frac{1}{\overline{\chi}_{T_+}}\|R_{T_+}^{(1)}(\mathbf{j_H})\|_{0,T_+}^2 + \frac{1}{\overline{\kappa}_{T_+}}\|R_{T_+}^{(2)}(\mathbf{j_H})\|_{0,T_+}^2\Big) + \\ + \frac{h_{T_-}^2}{m_-}\Big(\frac{1}{\overline{\chi}_{T_-}}\|R_{T_-}^{(1)}(\mathbf{j_H})\|_{0,T_-}^2 + \frac{1}{\overline{\kappa}_{T_-}}\|R_{T_-}^{(2)}(\mathbf{j_H})\|_{0,T_-}^2\Big) , \tag{2.5}$$

where $\overline{\chi}_{T_\pm} := |T_\pm|^{-1}\int_{T_\pm}\chi\,dx, \overline{\kappa}_{T_\pm} := |T_\pm|^{-1}\int_{T_\pm}\kappa\,dx$ and

$$m_\pm \;:=\; \mathrm{card}(\{F \in \mathcal{F}_H(\Omega) \mid F \cap \mathcal{F}_H(T_\pm) \ne \emptyset\}) .$$

Moreover, we define $\eta_F^{(2)}$ by means of

$$(\eta_F^{(2)})^2 \;:=\; h_F\Big(\frac{1}{\overline{\chi}_F}\|R_F^{(1)}(\mathbf{j_H})\|_{0,F}^2 + \frac{1}{\overline{\kappa}_F}\|R_F^{(2)}(\mathbf{j_H})\|_{0,F}^2\Big) , \tag{2.6}$$

where $\overline{\chi}_F := (\overline{\chi}_{T_+} + \overline{\chi}_{T_-})/2$ and $\overline{\kappa}_F := (\overline{\kappa}_{T_+} + \overline{\kappa}_{T_-})/2$.

We set

$$\eta_H^2 \;:=\; \sum_{F\in\mathcal{F}_H(\Omega)} \eta_{H,F}^2 \quad , \quad \eta_{H,F}^2 \;:=\; (\eta_{H,F}^{(1)})^2 + (\eta_{H,F}^{(2)})^2 . \tag{2.7}$$

The convergence analysis further involves the oscillations

$$osc_H^2 \;:=\; \sum_{F\in\mathcal{F}_H(\Omega)} osc_{H,F}^2 \quad , \quad osc_{H,F}^2 \;:=\; (osc_{H,F}^{(1)})^2 \;+\; (osc_{H,F}^{(2)})^2 . \tag{2.8}$$

Here, $osc_{H,F}^{(\nu)}, 1 \le \nu \le 2$, are given by

$$(osc_{H,F}^{(1)})^2 := \tag{2.9}$$
$$\frac{h_{T_+}^2}{m_+}\big(\|R_{T_+}^{(1)}(\mathbf{j_H}) - \overline{R}_{T_+}^{(1)}(\mathbf{j_H})\|_{0,T_+}^2 + \|R_{T_+}^{(2)}(\mathbf{j_H}) - \overline{R}_{T_+}^{(2)}(\mathbf{j_H})\|_{0,T_+}^2\big)$$
$$+\; \frac{h_{T_-}^2}{m_-}\big(\|R_{T_-}^{(1)}(\mathbf{j_H}) - \overline{R}_{T_-}^{(1)}(\mathbf{j_H})\|_{0,T_-}^2 + \|R_{T_-}^{(2)}(\mathbf{j_H}) - \overline{R}_{T_-}^{(2)}(\mathbf{j_H})\|_{0,T_-}^2\big) ,$$
$$(osc_{H,F}^{(2)})^2 := \tag{2.10}$$
$$h_F\Big(\frac{1}{\overline{\chi}_F}\|R_F^{(1)}(\mathbf{j_H}) - \overline{R}_F^{(1)}(\mathbf{j_H})\|_{0,F}^2 + \frac{1}{\overline{\kappa}_F}\|R_F^{(2)}(\mathbf{j_H}) - \overline{R}_F^{(2)}(\mathbf{j_H})\|_{0,F}^2\Big)$$

where

$$\overline{R}^{(\nu)}_{T_\pm}(\mathbf{j_H}) \;:=\; |T_\pm|^{-1} \int\limits_{T_\pm} R^{(\nu)}_{T_\pm}(\mathbf{j_H})\; dx \;,\; \overline{R}^{(\nu)}_{F}(\mathbf{j_H}) \;:=\; |F|^{-1} \int\limits_{F} R^{(\nu)}_{F}(\mathbf{j_H})\; d\sigma \;,\; 1 \le \nu \le 2 \;.$$

The subsequent step MARK is devoted to the selection of interior faces $F \in \mathcal{F}_H(\Omega)$, $F = T_+ \cap T_-, T_\pm \in \mathcal{T}_H$, and adjacent elements from $\mathcal{T}_H$ for refinement. In particular, given two universal constants $0 < \Theta_\nu < 1, 1 \le \nu \le 2$, we select subsets $\mathcal{M}^{(\nu)} \subset \mathcal{F}_H(\Omega)$ such that

$$\Theta_1 \sum_{F \in \mathcal{F}_H(\Omega)} \eta^2_{H,F} \;\le\; \sum_{F \in \mathcal{M}^{(1)}} \eta^2_{H,F} \;, \tag{2.11}$$

$$\Theta_2 \sum_{F \in \mathcal{F}_H(\Omega)} osc^2_{H,F} \le \sum_{F \in \mathcal{M}^{(2)}} osc^2_{H,F} \;. \tag{2.12}$$

These so-called bulk criteria (2.11),(2.12) can be realized by a greedy algorithm (cf., e.g., [9, 17, 31]).

In the final step REFINE of the adaptive loop (1.11), for a face $F \in \mathcal{M}^{(1)} \cup \mathcal{M}^{(2)}, F = T_+ \cap T_-, T_\pm \in \mathcal{T}_H$, we refine all elements $T' \in \mathcal{T}_H$ with $\mathcal{F}_H(T') \cap \mathcal{F}_H(T_\pm) \neq \emptyset$ such that all such T' and all faces $F \in \mathcal{F}_H(T') \cap \mathcal{F}_H(T_\pm)$ contain a node in their interior. For a realization of this so-called interior node property we refer to [25]. Eventually, further refinements are necessary to guarantee that the resulting refined mesh $\mathcal{T}_h$ is geometrically conforming such that the edge element spaces $\mathbf{Nd_{1,0}}(\Omega; \mathcal{T}_H)$ and $\mathbf{Nd_{1,0}}(\Omega; \mathcal{T}_h)$ are nested.

If we proceed according to the steps SOLVE, ESTIMATE, MARK, and REFINE as specified above, we can prove the following convergence result:

Theorem 2.1 *Let* $\mathbf{j_H}$ *and* $\mathbf{j_h}$ *be the edge element approximations of the solution* $\mathbf{j}$ *of* (1.9) *with respect to the triangulation* $\mathcal{T}_H$ *and its refinement* $\mathcal{T}_h$ *generated according to the steps MARK and REFINE of the adaptive loop. Let further* η_H *and* osc_H *be the residual-type a posteriori error estimator and the oscillations given by* (2.7) *and* (2.8) *respectively. Then, there exist constants* $0 < \rho < 1$ and $C > 0$, *depending on the data* χ, κ, it on the constants $\Theta_\nu, 1 \le \nu \le 2$, *in* (2.11),(2.12), *and on the shape* *regularity of the triangulations, such that*

$$|||\mathbf{j} - \mathbf{j_h}|||^2 \ + \ C \ osc_h^2 \ \leq \ \rho \ \left(|||\mathbf{j} - \mathbf{j_H}|||^2 \ + \ C \ osc_H^2 \right) \ . \tag{2.13}$$

The proof of Theorem 2.1 hinges on the reliability of the estimator η_H and on an error reduction and an oscillation reduction result. As far as the reliability is concerned, we note that a residual-type a posteriori error estimator similar to (2.7) has been derived and analyzed in [7]. In particular, its reliability has been shown by means of a Scott/Zhang-type interpolation operator which, however, required some additional regularity of the solution, namely $\mathbf{j} \in \mathbf{H_0}(\mathbf{curl};\Omega) \cap \mathbf{H^1}(\Omega)$. This result has been significantly improved in [30] relying on a Clément-type commuting quasi-interpolation operator $\mathbf{\Pi_H} : \mathbf{H_0}(\mathbf{curl};\Omega) \rightarrow \mathbf{Nd_{1,0}}(\Omega, \mathcal{T}_H)$ with the property: For every $\mathbf{q} \in \mathbf{H_0}(\mathbf{curl};\Omega)$ there exist $\varphi \in H_0^1(\Omega)$ and $\mathbf{z} \in \mathbf{H_0^1}(\Omega)$ such that

$$\mathbf{q} \ - \ \mathbf{\Pi_H q} \ = \ \mathbf{grad}(\varphi) \ + \ \mathbf{z} \ , \tag{2.14}$$

$$h_T^{-1} \ \|\varphi\|_{0,T} \ + \ \|\mathbf{grad}(\varphi)\|_{0,T} \ \lesssim \ \|\mathbf{q}\|_{0,\omega_T} \quad , \quad T \in \mathcal{T}_H \ , \tag{2.15}$$

$$h_T^{-1} \ \|\mathbf{z}\|_{0,T} \ + \ \|\mathbf{grad}(\mathbf{z})\|_{0,T} \ \lesssim \ \|\mathbf{curl}(\mathbf{q})\|_{0,\omega_T} \quad , \quad T \in \mathcal{T}_H \ , \tag{2.16}$$

where $\omega_T := \cup\{T' \in \mathcal{T}_H | \mathcal{N}_H(T') \cap \mathcal{N}_H(T) \neq \emptyset\}$.

Using (2.14)-(2.16), reliability of η_H can be shown:

Theorem 2.2(cf. [30]) *For the estimator η_H as given by* (2.7) *there holds*

$$|||\mathbf{j} - \mathbf{j_H}|||^2 \ \lesssim \ \eta_H^2 \ . \tag{2.17}$$

3. Error reduction. The error reduction property asserts that, up to the oscillations osc_H, the energy norm of the difference between the fine and coarse mesh approximations $\mathbf{j_h} \in \mathbf{Nd_{1,0}}(\Omega, \mathcal{T}_h)$ and $\mathbf{j_H} \in \mathbf{Nd_{1,0}}(\Omega, \mathcal{T}_H)$ is bounded from below by the error estimator.

Theorem 3.1 *There exists a constant $C_1 > 0$, depending only on the data χ, κ, the constant Θ_1 in the bulk criterion* (2.11), *and on the shape regularity of the* *triangulations such that*

$$\eta_H^2 \;\le\; C_1\ \left(|||\mathbf{j_h} - \mathbf{j_H}|||^2 \;+\; osc_H^2 \right) \,. \tag{3.1}$$

The proof of Theorem 3.1 follows from a series of lemmas providing upper bounds for the local components of the error estimator and thus establishing what is known as discrete local efficiency of the error estimator. The first two results deal with $\eta_{H,F}^{(1)}$.

Lemma 3.1 *Assume that $T_\pm \in \mathcal{T}_H$ are refined triangles. Then, there holds*

$$\begin{aligned} &(m_\pm \overline{\chi}_{T_\pm})^{-1} h_{T_\pm}^2 \|R_{T_\pm}^{(1)}(\mathbf{j_H})\|_{0,T_\pm}^2 \;\lesssim \qquad\qquad (3.2)\\ &\lesssim\; \|\mathbf{j_h} - \mathbf{j_H}\|_{curl,T_\pm}^2 + m_\pm^{-1} h_{T_\pm}^2 \|R_{T_\pm}^{(1)}(\mathbf{j_H}) - \overline{R}_{T_\pm}^{(1)}(\mathbf{j_H})\|_{0,T_\pm}^2 \,. \end{aligned}$$

Proof. The triangle and Cauchy Schwarz inequalities readily give

$$\begin{aligned} &(m_\pm \overline{\chi}_{T_\pm})^{-1} h_{T_\pm}^2 \|R_{T_\pm}^{(1)}(\mathbf{j_H})\|_{0,T_\pm}^2 \;\le \qquad\qquad (3.3)\\ &\le\; 2(m_\pm \overline{\chi}_{T_\pm})^{-1} h_{T_\pm}^2\ \left(\|\overline{R}_{T_\pm}^{(1)}\|_{0,T_\pm}^2 + \|R_{T_\pm}^{(1)}(\mathbf{j_H}) - \overline{R}_{T_\pm}^{(1)}(\mathbf{j_H})\|_{0,T_\pm}^2 \right) \,. \end{aligned}$$

We denote by $a_{h,T_\pm}^{int} \in \mathcal{T}_h(\mathrm{int}(T_\pm))$ an interior point in $T_\pm$ and refer to

$$D_{h,T_\pm}^a \;:=\; \bigcup \{T' \in \mathcal{T}_h(T_\pm) \mid a_{h,T_\pm}^{int} \in \mathcal{N}_h(T')\}$$

as the union of all fine mesh triangles having $a_{h,T_\pm}^{int}$ as a common vertex. Moreover, we denote by $E_{h,\nu_\pm}^a \in \mathcal{E}_h(\mathrm{int}(D_{h,T_\pm}^a)), 1 \le \nu_\pm \le \nu_\pm^a, \nu_\pm^a \ge 3$, the interior edges in $D_{h,T_\pm}^a \subset T_\pm$. We choose $\mathbf{q_{h,T_\pm}^a} := \sum_{\nu_\pm=1}^{\nu_\pm^a} \alpha_{\nu_\pm} \boldsymbol{\varphi}_{\mathbf{h},\nu_\pm}$ as a linear combination of the basis functions $\boldsymbol{\varphi}_{\mathbf{h},\nu_\pm} \in \mathbf{Nd_{1,0}}(D_{h,T_\pm}^a;\mathcal{T}_h)$ associated with the interior edges such that

$$\begin{aligned} &(m_\pm \overline{\chi}_{T_\pm})^{-1} h_\pm^2 \|\overline{R}_{T_\pm}^{(1)}(\mathbf{j_H})\|_{0,T_\pm}^2 \;=\; h_\pm^2\ \left(\overline{R}_{T_\pm}^{(1)}(\mathbf{j_H}), \mathbf{q_{h,T_\pm}^a}\right)_{0,T_\pm} \;= \qquad (3.4)\\ &=\; h_\pm^2\ (R_{T_\pm}^{(1)}(\mathbf{j_H}), \mathbf{q_{h,T_\pm}^a})_{0,T_\pm} \;+\; h_\pm^2\ (\overline{R}_{T_\pm}^{(1)}(\mathbf{j_H}) - R_{T_\pm}^{(1)}(\mathbf{j_H}), \mathbf{q_{h,T_\pm}^a})_{0,T_\pm} \,,\\ &\sum_{\nu_\pm=1}^{\nu_\pm^a} |\alpha_{\nu_\pm}| \;\le\; (m_\pm \overline{\chi}_{T_\pm})^{-1/2}\ |\overline{R}_{T_\pm}^{(1)}(\mathbf{j_H})| \,. \qquad (3.5) \end{aligned}$$

By means of (2.3) and in view of $\boldsymbol{\pi}_{\mathbf{t}}(\mathbf{q_{h,T_\pm}^a})|_{\partial D_{h,T_\pm}^a} = 0$, Stokes' theorem gives

$$\begin{aligned} &h_{T_\pm}^2 (R_{T_\pm}^{(1)}(\mathbf{j_H}), \mathbf{q_{h,T_\pm}^a})_{0,T_\pm} = h_{T_\pm}^2 (\mathbf{curl}(\chi \mathbf{curl}(\mathbf{j_H})) + \kappa \mathbf{j_H} - \mathbf{f}, \mathbf{q_{h,T_\pm}^a})_{0,T_\pm} \;= (3.6)\\ &=\; h_{T_\pm}^2 \left((\chi \mathbf{curl}(\mathbf{j_H}), \mathbf{curl}(\mathbf{q_{h,T_\pm}^a}))_{0,T_\pm} + (\kappa \mathbf{j_H} - \mathbf{f}, \mathbf{q_{h,T_\pm}^a})_{0,T_\pm} \right) \,. \end{aligned}$$

Further, we take advantage of the fact that $\mathbf{q}^{\mathbf{a}}_{\mathbf{h},\mathbf{T}_\pm}$ is an admissible test function in (1.10) whence

$$(\chi \mathbf{curl}(\mathbf{j_h}), \mathbf{curl}(\mathbf{q}^{\mathbf{a}}_{\mathbf{h},\mathbf{T}_\pm}))_{0,T_\pm} + (\kappa \mathbf{j_h} - \mathbf{f}, \mathbf{q}^{\mathbf{a}}_{\mathbf{h},\mathbf{T}_\pm})_{0,T_\pm} \ = \ 0 \ . \tag{3.7}$$

Combining (3.6),(3.7) and using (3.5) as well as

$$\|\boldsymbol{\varphi}_{\mathbf{h},\nu_\pm}\|_{0,T_\pm} \ \lesssim \ h_{T_\pm} \quad , \quad \|\mathbf{curl}(\boldsymbol{\varphi}_{\mathbf{h},\nu_\pm})\|_{0,T_\pm} \ \lesssim \ 1 \ ,$$

we obtain

$$\begin{aligned} & h^2_{T_\pm} \ |(R^{(1)}_{T_\pm}(\mathbf{j_H}), \mathbf{q}^{\mathbf{a}}_{\mathbf{h},\mathbf{T}_\pm})_{0,T_\pm}| \ = \\ & = \ h^2_{T_\pm} \ \big|\big((\chi \mathbf{curl}(\mathbf{j_H} - \mathbf{j_h}), \mathbf{curl}(\mathbf{q}^{\mathbf{a}}_{\mathbf{h},\mathbf{T}_\pm}))_{0,T_\pm} + (\kappa(\mathbf{j_H} - \mathbf{j_h}), \mathbf{q}^{\mathbf{a}}_{\mathbf{h},\mathbf{T}_\pm})_{0,T_\pm}\big)\big| \ \lesssim \\ & \lesssim \ \big(h_{T_\pm} \ \|\chi\|_{\infty,T_\pm} \ \|\mathbf{curl}(\mathbf{j_H} - \mathbf{j_h})\|_{0,T_\pm} + h^2_{T_\pm} \ \|\kappa\|_{\infty,T_\pm} \ \|\mathbf{j}_H - \mathbf{j_h}\|_{0,T_\pm}\big) \|\overline{R}^{(1)}_{T_\pm}(\mathbf{j_H})\|_{0,T_\pm} \ \lesssim \\ & \lesssim \ \|\mathbf{j_H} - \mathbf{j_h}\|_{curl,T_\pm} \ (m_\pm \overline{\chi}_{T_\pm})^{-1/2} \|\overline{R}^{(1)}_{T_\pm}(\mathbf{j_H})\|_{0,T_\pm} \ . \end{aligned} \tag{3.8}$$

Finally, for the second term on the right-hand side in (3.4) we get

$$\begin{aligned} & h^2_{T_\pm} |(\overline{R}^{(1)}_{T_\pm}(\mathbf{j_H}) - R^{(1)}_{T_\pm}(\mathbf{j_H}), \mathbf{q}^{\mathbf{a}}_{\mathbf{h},\mathbf{T}_\pm})_{0,T_\pm}| \ \lesssim \\ & \lesssim \ h_{T_\pm} \|\overline{R}^{(1)}_{T_\pm}(\mathbf{j_H}) - R^{(1)}_{T_\pm}(\mathbf{j_H})\|_{0,T_\pm} (m_\pm \overline{\chi}_{T_\pm})^{-1/2} \|\overline{R}^{(1)}_{T_\pm}(\mathbf{j_H})\|_{0,T_\pm} \ . \end{aligned} \tag{3.9}$$

The assertion follows readily from (3.3),(3.8) and (3.9). *q.e.d.*

Lemma 3.2. *For refined triangles $T_\pm \in \mathcal{T}_H$ there holds*

$$\begin{aligned} & (m_\pm \bar{\kappa}_{T_\pm})^{-1} h^2_{T_\pm} \|R^{(2)}_{T_\pm}(\mathbf{j_H})\|^2_{0,T_\pm} \ \lesssim \\ & \lesssim \ \|\mathbf{j_h} - \mathbf{j_H}\|^2_{0,T_\pm} + m_\pm^{-1} h^2_{T_\pm} \|R^{(2)}_{T_\pm}(\mathbf{j_H}) - \overline{R}^{(2)}_{T_\pm}(\mathbf{j_H})\|^2_{0,T_\pm} . \end{aligned} \tag{3.10}$$

Proof. Obviously, we have

$$\begin{aligned} & (m_\pm \overline{\kappa}_{T_\pm})^{-1} h^2_{T_\pm} \|R^{(2)}_{T_\pm}(\mathbf{j_H})\|^2_{0,T_\pm} \ \leq \\ & \leq \ 2(m_\pm \overline{\kappa}_{T_\pm})^{-1} h^2_{T_\pm} \ \big(\|\overline{R}^{(2)}_{T_\pm}(\mathbf{j_H})\|^2_{0,T_\pm} + \|R^{(2)}_{T_\pm}(\mathbf{j_H}) - \overline{R}^{(2)}_{T_\pm}(\mathbf{j_H})\|^2_{0,T_\pm} . \end{aligned} \tag{3.11}$$

In order to derive an upper bound for the first term on the right-hand side in (3.11), let $a^{int}_{T_\pm} \in \mathcal{N}_h(T_\pm)$ be an interior nodal point and $T^{'}_{\nu_\pm} \in \mathcal{T}_{T_\pm}$ such that $a^{int}_{T_\pm} \in \mathcal{N}_h(T^{'}_{\nu_\pm}), 1 \leq$

$\nu_\pm \le \nu_\pm^a$. We choose $\varphi_{h,T_\pm}^a \in S_{1,0}(\Omega;\mathcal{T}_h)$ as a multiple of the P1 conforming nodal basis function with supporting point $a_{T_\pm}^{int}$ according to

$$\varphi_{h,T_\pm}^a(a_{T_\pm}^{int}) \;=\; \big(\overline{\kappa}_{T_\pm}\sum_{\nu_\pm=1}^{\nu_\pm^a}|T'_{\nu_\pm}|\big)^{-1}\big(\nu_\pm^a|T_\pm|\big)\;\bar{R}_{T_\pm}^{(2)}(\mathbf{j_H})\;.$$

Due to the shape regularity of the triangulations, we have

$$\|\varphi_{h,T_\pm}^a(a_{T_\pm}^{int})\|_{0,T_\pm} \lesssim (m_\pm\bar{\kappa}_{T,\pm})^{-1}\;\|\bar{R}_{T_\pm}^{(2)}\|_{0,T_\pm}(\mathbf{j_H})\;, \tag{3.12}$$

$$\|\mathbf{grad}(\varphi_{h,T_\pm}^a(a_{T_\pm}^{int}))\|_{0,T_\pm} \lesssim (m_\pm\bar{\kappa}_{T_\pm})^{-1}\;|T_\pm|^{-1/2}\;\|\bar{R}_{T_\pm}^{(2)}(\mathbf{j_H})\|_{0,T_\pm}\;. \tag{3.13}$$

Due to the definition of $\varphi_{h,T_\pm}^a$ we have

$$\begin{aligned}(m_\pm\overline{\kappa}_{T_\pm})^{-1}h_\pm^2\|\bar{R}_{T_\pm}^{(2)}(\mathbf{j_H})\|_{0,T_\pm}^2 \;&=\; h_\pm^2\;\big(\overline{R}_{T_\pm}^{(2)}(\mathbf{j_H}),\varphi_{h,T_\pm}^a)_{0,T_\pm} \;= \\ =\; h_\pm^2\;(R_{T_\pm}^{(2)}(\mathbf{j_H}),\varphi_{h,T_\pm}^a)_{0,T_\pm} \;&+\; h_\pm^2\;(\overline{R}_{T_\pm}^{(2)}(\mathbf{j_H})-R_{T_\pm}^{(2)}(\mathbf{j_H}),\varphi_{h,T_\pm}^a)_{0,T_\pm}\;.\end{aligned} \tag{3.14}$$

In view of (3.12), we obtain

$$\begin{aligned}&h_\pm^2\;|(\overline{R}_{T_\pm}^{(2)}(\mathbf{j_H})-R_{T_\pm}^{(2)}(\mathbf{j_H}),\varphi_{h,T_\pm}^a)_{0,T_\pm}|\;\le \\ &\le\; h_\pm^2\;\|\overline{R}_{T_\pm}^{(2)}(\mathbf{j_H})-R_{T_\pm}^{(2)}(\mathbf{j_H})\|_{0,T_\pm}\;\|\varphi_{h,T_\pm}^a\|_{0,T_\pm}\;\lesssim \\ &\lesssim\;(m_\pm\kappa_0)^{-1/2}h_\pm\;\|\overline{R}_{T_\pm}^{(2)}(\mathbf{j_H})-R_{T_\pm}^{(2)}(\mathbf{j_H})\|_{0,T_\pm}\;(m_\pm\overline{\kappa}_{T_\pm})^{-1/2}h_\pm\;\|\overline{R}_{T_\pm}^{(2)}(\mathbf{j_H})\|_{0,T_\pm}\;.\end{aligned} \tag{3.15}$$

Moreover, observing $\varphi_{h,T_\pm}^a)_{0,T_\pm}|_{\partial T_\pm}=0$, Green's formula implies

$$\begin{aligned}&|T_\pm\;(R_{T_\pm}^{(2)}(\mathbf{j_H}),\varphi_{h,T_\pm}^a)_{0,T_\pm}\;= \\ &=\;|T_\pm|\;(\mathrm{div}(\kappa\mathbf{j_H})-\mathrm{div}(\mathbf{f}),\varphi_{h,T_\pm}^a)_{0,T_\pm}\;=\;(\kappa\mathbf{j_H}-\mathbf{f},\mathbf{grad}(\varphi_{h,T_\pm}^a))_{0,T_\pm}\;.\end{aligned} \tag{3.16}$$

On the other hand, since $\mathbf{grad}(\varphi_{h,T_\pm}^a)$ is an admissible test function in (1.10), we have

$$(\kappa\mathbf{j_h},\mathbf{grad}(\varphi_{h,T_\pm}^a))_{0,T_\pm}\;=\;(\mathbf{f},\mathbf{grad}(\varphi_{h,T_\pm}^a))_{0,T_\pm}\;. \tag{3.17}$$

Consequently, combining (3.16) and (3.17) and taking advantage of (3.13), it follows that

$$\begin{aligned}&|T_\pm\;|(R_{T_\pm}^{(2)}(\mathbf{j_H}),\varphi_{h,T_\pm}^a)_{0,T_\pm}|\;=\;(\kappa(\mathbf{j_h}-\mathbf{j_H},\mathbf{grad}(\varphi_{h,T_\pm}^a))_{0,T_\pm}|\;\lesssim \\ &\lesssim\;(m_\pm\overline{\kappa}_{T_\pm})^{-1}|T_\pm|^{1/2}\;\|\kappa\|_{\infty,T_\pm}\;\|\kappa(\mathbf{j_h}-\mathbf{j_H}\|_{0,T_\pm}\;\|\overline{R}_{T_\pm}^{(2)}(\mathbf{j_H})\|_{0,T_\pm}\;\lesssim \\ &\lesssim\;\kappa_0^{-1}\;\|\kappa\|_{\infty,T_\pm}\;\|\kappa(\mathbf{j_h}-\mathbf{j_H}\|_{0,T_\pm}\;(m_\pm\overline{\kappa}_{T_\pm})^{-1/2}|T_\pm|^{1/2}\;\|\overline{R}_{T_\pm}^{(2)}(\mathbf{j_H})\|_{0,T_\pm}\;.\end{aligned} \tag{3.18}$$

The estimate (3.10) follows from (3.11),(3.14) and (3.18). *q.e.d.*

The following two results are concerned with an upper bound for $\eta^{(2)}_{H,F}$.

Lemma 3.3 *For a refined face $F \in \mathcal{F}_H$ there holds*

$$\overline{\chi}_F^{-1}\ h_F\ \|R_F^{(1)}(\mathbf{j_H})\|^2_{0,F}\ \lesssim\ \|\mathbf{j_h} - \mathbf{j_H}\|^2_{curl,\omega_F}\ + \tag{3.19}$$
$$+ \sum_{T_\pm \in \mathcal{T}_H(\omega_F)} h^2_{T_\pm}\ \|R^{(1)}_{T_\pm}(\mathbf{j_H})\|^2_{0,T_\pm}\ +\ h_F\ \|R_F^{(1)}(\mathbf{j_H}) - \overline{R}_F^{(1)}(\mathbf{j_H})\|^2_{0,F}\ .$$

Proof. We have

$$\overline{\chi}_F^{-1}\ h_F\ \|R_F^{(1)}(\mathbf{j_H})\|^2_{0,F}\ \le \tag{3.20}$$
$$\le\ 2\ \overline{\chi}_F^{-1}\ h_F\ \left(\|\overline{R}_F^{(1)}(\mathbf{j_H})\|^2_{0,F} + \|R_F^{(1)}(\mathbf{j_H}) - \overline{R}_F^{(1)}(\mathbf{j_H})\|^2_{0,F}\right)\ .$$

Let $a^{int}_{h,F} \in \mathcal{N}_h(F)$ be an interior point and denote by

$$D^a_{h,\omega_F}\ :=\ \bigcup \{T' \in \mathcal{T}_h(\omega_F)\ |\ a^{int}_{h,F} \in \mathcal{N}_h(T')\}$$

the union of all fine mesh elements sharing $a^{int}_{h,F}$ as a common vertex. We denote by $E_{h,\nu} \in \mathcal{E}_h(F), 1 \le \nu \le \nu^a_F$, the interior edges in $D^a_{h,\omega_F} \cap F$. Then, we choose $\mathbf{q^a_{h,F}} := \sum_{\nu=1}^{\nu^a_F} \alpha_\nu \boldsymbol{\varphi}_{\mathbf{h},\boldsymbol{\nu}}$ as a linear combination of the basis functions $\boldsymbol{\varphi}_{\mathbf{h},\boldsymbol{\nu}} \in \mathbf{Nd_{1,0}}(D^a_{h,\omega_F}, \mathcal{T}_h)$ associated with the interior edges $E_{h,\nu}$ such that

$$\overline{\chi}_F^{-1}\ h_F\ \|\overline{R}_F^{(1)}(\mathbf{j_H})\|^2_{0,F}\ =\ h_F\ (\overline{R}_F^{(1)}(\mathbf{j_H}), \boldsymbol{\pi}_\mathbf{t}(\mathbf{q^a_{h,F}}))_{0,F}\ = \tag{3.21}$$
$$=\ h_F\ \left((R_F^{(1)}(\mathbf{j_H}), \boldsymbol{\pi}_\mathbf{t}(\mathbf{q^a_{h,F}}))_{0,F}\ +\ (\overline{R}_F^{(1)}(\mathbf{j_H}) - R_F^{(1)}(\mathbf{j_H}), \boldsymbol{\pi}_\mathbf{t}(\mathbf{q^a_{h,F}}))_{0,F}\right)\ ,$$
$$\sum_{\nu=1}^{\nu^a_F} |\alpha_\nu|\ \lesssim\ \overline{\chi}_F^{-1/2}\ |\overline{R}_F^{(1)}(\mathbf{j_H})|\ . \tag{3.22}$$

Recalling (2.5) and observing $\mathbf{q^a_{h,F}}|_{\partial D^a_{h,\omega_F}} = 0$, Stokes' theorem gives

$$h_F\ (R_F^{(1)}(\mathbf{j_H}), \boldsymbol{\pi}_\mathbf{t}(\mathbf{q^a_{h,F}}))_{0,F}\ =\ h_F\ ([\chi \mathbf{curl}(\mathbf{j_H}) \wedge \mathbf{n_F}]_F, \boldsymbol{\pi}_\mathbf{t}(\mathbf{q^a_{h,F}}))_{0,F}\ = \tag{3.23}$$
$$=\ h_F\ \left((\chi \mathbf{curl}(\mathbf{j_H}), \mathbf{curl}(\mathbf{q^a_{h,F}}))_{0,\omega_F}\ +\ (\kappa \mathbf{j_H} - \mathbf{f}, \mathbf{q^a_{h,F}})_{0,\omega_F}\ -\right.$$
$$\left.-\ \sum_{T_\pm \in \mathcal{T}_H(\omega_F)} (R^{(1)}_{T_\pm}(\mathbf{j_H}), \mathbf{q^a_{h,F}})_{0,T_\pm}\right)\ .$$

Since $\mathbf{q^a_{h,F}}$ is an admissible test function in (1.10), we have

$$(\chi \mathbf{curl}(\mathbf{j_h}), \mathbf{curl}(\mathbf{q^a_{h,F}}))_{0,\omega_F}\ +\ (\kappa \mathbf{j_h} - \mathbf{f}, \mathbf{q^a_{h,F}})_{0,\omega_F}\ =\ 0\ . \tag{3.24}$$

Hence, subtracting (3.24) from (3.23) and using (3.22) as well as

$$\|\boldsymbol{\varphi}_{\mathbf{h},\boldsymbol{\nu}}\|_{0,\omega_F} \lesssim h_F \quad , \quad \|\mathbf{curl}(\boldsymbol{\varphi}_{\mathbf{h},\boldsymbol{\nu}})\|_{0,\omega_F} \lesssim 1 \quad , \quad 1 \le \nu \le \nu_F^a \ ,$$

it follows that

$$\begin{aligned} & h_F \ |(R_F^{(1)}(\mathbf{j_H}), \boldsymbol{\pi}_\mathbf{t}(\mathbf{q^a_{h,F}}))_{0,F}| \ \lesssim \qquad (3.25) \\ & \lesssim \ \big(\|\chi\|_{\infty,\omega_F} \ \|\mathbf{curl}(\mathbf{j_H} - \mathbf{j_h})\|_{0,\omega_F} \ + \ h_F \ \|\kappa\|_{\infty,\omega_F} \ \|\mathbf{j_H} - \mathbf{j_h}\|_{0,\omega_F} \ + \\ & + \ h_F \sum_{T_\pm \in \mathcal{T}_H(\omega_F)} \|R_{T_\pm}^{(1)}(\mathbf{j_H})\|_{0,T_\pm}\big) \ \overline{\chi}_F^{-1/2} h_F^{1/2} \|\overline{R}_F^{(1)}(\mathbf{j_H})\|_{0,F} \ . \end{aligned}$$

Using (3.22) and

$$\|\boldsymbol{\pi}_\mathbf{t}(\boldsymbol{\varphi}_{\mathbf{h},\boldsymbol{\nu}})\|_{0,F} \ \lesssim \ h_F^{1/2} \quad , \quad 1 \le \nu \le \nu_F^a \ ,$$

for the second term on the right-hand side in (3.21) we obtain

$$\begin{aligned} & h_F |(\overline{R}_F^{(1)}(\mathbf{j_H}) - R_F^{(1)}(\mathbf{j_H}), \boldsymbol{\pi}_\mathbf{t}(\mathbf{q^a_{h,F}}))_{0,F}| \ \lesssim \qquad (3.26) \\ & \lesssim \ h_F^{1/2} \|R_F^{(1)}(\mathbf{j_H}) - \overline{R}_F^{(1)}(\mathbf{j_H})\|_{0,F} \overline{\chi}_F^{-1/2} h_F^{1/2} \|\overline{R}_F^{(1)}(\mathbf{j_H})\|_{0,F} \ . \end{aligned}$$

We conclude by combining (3.20),(3.25) and (3.26). *q.e.d.*

Lemma 3.4. *Let $F \in \mathcal{F}_H$ be a refined face. Then, there holds*

$$\begin{aligned} & \overline{\kappa}_F^{-1} \ h_F \ \|R_F^{(2)}(\mathbf{j_H})\|_{0,F}^2 \ \lesssim \ \|\mathbf{j_h} - \mathbf{j_H}\|_{0,\omega_F}^2 \ + \qquad (3.27) \\ & + \sum_{T_\pm \in \mathcal{T}_H(\omega_F)} h_{T_\pm}^2 \ \|R_{T_\pm}^{(2)}(\mathbf{j_H})\|_{0,T_\pm}^2 \ + \ h_F \ \|R_F^{(2)}(\mathbf{j_H}) - \overline{R}_F^{(2)}(\mathbf{j_H})\|_{0,F}^2 \ . \end{aligned}$$

Proof. We have

$$\begin{aligned} & \overline{\kappa}_F^{-1} \ h_F \ \|R_F^{(2)}(\mathbf{j_H})\|_{0,F}^2 \ \le \qquad (3.28) \\ & \le \ 2 \ \overline{\kappa}_F^{-1} \ h_F \ \big(\|\overline{R}_F^{(2)}(\mathbf{j_H})\|_{0,F}^2 + \|R_F^{(2)}(\mathbf{j_H}) - \overline{R}_F^{(2)}(\mathbf{j_H})\|_{0,F}^2\big) \ . \end{aligned}$$

We choose $\varphi_{h,F}^a \in S_{1,0}(\Omega; \mathcal{T}_h)$ as a multiple of the P1 conforming nodal basis function with supporting interior nodal point $a_{h,F}^{int} \in \mathcal{N}_h(F)$ such that

$$\varphi_{h,F}^a(a_{h,F}^{int}) \ = \ \Big(\overline{\kappa}_F \sum_{\nu=1}^{\nu_F^a} |F_\nu'|\Big)^{-1} \ \big(\nu_F^a |F|\big) \ \overline{R}_F^{(2)}(\mathbf{j_H}) \ , \qquad (3.29)$$

where $F'_\nu \in \mathcal{F}_h(F), a_{h,F}^{int} \in \mathcal{N}_h(F'_\nu), 1 \le \nu \le \nu_F^a$. Due to (3.29) and the shape regularity of the triangulations, there holds

$$\|\varphi_{h,F}^a\|_{0,F} \lesssim \overline{\kappa}_F^{-1} \ \|\overline{R}_F^{(2)}(\mathbf{j_H})\|_{0,F} \ , \tag{3.30}$$

$$\|\varphi_{h,F}^a\|_{0,T_\pm} \lesssim \overline{\kappa}_F^{-1} \ h_F^{1/2} \ \|\overline{R}_F^{(2)}(\mathbf{j_H})\|_{0,F} \ , \ T_\pm \in \mathcal{T}_H(\omega_F) \ , \tag{3.31}$$

$$\|\mathbf{grad}(\varphi_{h,F}^a)\|_{0,T_\pm} \lesssim \overline{\kappa}_F^{-1} \ h_F^{-1/2} \ \|\overline{R}_F^{(2)}(\mathbf{j_H})\|_{0,F} \ , \ T_\pm \in \mathcal{T}_H(\omega_F) \ . \tag{3.32}$$

Moreover, for the first term on the right-hand side in (3.28) it follows from (3.29) that

$$\begin{aligned} &\overline{\kappa}_F^{-1} \ h_F \ \|\overline{R}_F^{(2)}(\mathbf{j_H})\|_{0,F}^2 \ = \ h_F \ (\overline{R}_F^{(2)}(\mathbf{j_H}), \varphi_{h,F}^a)_{0,F} \ = \\ &= \ h_F \ (R_F^{(2)}(\mathbf{j_H}), \varphi_{h,F}^a)_{0,F} \ + \ h_F \ (\overline{R}_F^{(2)}(\mathbf{j_H}) - R_F^{(2)}(\mathbf{j_H}), \varphi_{h,F}^a)_{0,F} \ . \end{aligned} \tag{3.33}$$

In view of (2.4) and taking $\varphi_{h,F}^a|_{\partial\omega_F}$ into account, by partial integration we find

$$\begin{aligned} &h_F \ (R_F^{(2)}(\mathbf{j_H}), \varphi_{h,F}^a)_{0,F} \ = \ h_F \ ([\mathbf{n_F} \cdot (\kappa \mathbf{j_H} - \mathbf{f})]_F, \varphi_{h,F}^a)_{0,F} \ = \\ &= \ h_F \sum_{T_\pm \in \mathcal{T}_H(\omega_F)} \Big((\mathrm{div}(\kappa \mathbf{j_H}) - \mathrm{div}(\mathbf{f}), \varphi_{h,F}^a)_{0,T_\pm} + (\kappa \mathbf{j_H} - \mathbf{f}, \mathbf{grad}(\varphi_{h,F}^a))_{0,T_\pm} \Big) \ . \end{aligned} \tag{3.34}$$

Since $\mathbf{grad}(\varphi_{h,F}^a)$ is an admissible test function in (1.10), we have

$$(\kappa \mathbf{j_h}, \mathbf{grad}(\varphi_{h,F}^a))_{0,\omega_F} \ = \ (\mathbf{f}, \mathbf{grad}(\varphi_{h,F}^a))_{0,\omega_F} \ . \tag{3.35}$$

Hence, inserting (3.34) into (3.33) and using (3.30), (3.31) yields

$$\begin{aligned} &h_F \ |(R_F^{(2)}(\mathbf{j_H}), \varphi_{h,F}^a)_{0,F}| \ \le \ h_F |(\kappa \mathbf{j_H} - \mathbf{j_h}, \mathbf{grad}(\varphi_{h,F}^a))_{0,\omega_F}| \ + \\ &+ h_F \sum_{T_\pm \in \mathcal{T}_H(\omega_F)} |\big((\mathrm{div}(\kappa \mathbf{j_H}) - \mathrm{div}(\mathbf{f}), \varphi_{h,F}^a)_{0,T_\pm}| \ \lesssim \\ &\lesssim \ h_F \ \|\kappa\|_{\infty,\omega_F} \ \|\mathbf{j_h} - \mathbf{j_H}\|_{0,\omega_F} \ \|\mathbf{grad}(\varphi_{h,F}^a)\|_{0,\omega_F} \ + \\ &+ h_F \sum_{T_\pm \in \mathcal{T}_H(\omega_F)} \|\mathrm{div}(\kappa \mathbf{j_H}) - \mathrm{div}(\mathbf{f})\|_{0,T_\pm} \ \|\varphi_{h,F}^a\|_{0,T_\pm} \ . \end{aligned} \tag{3.36}$$

The estimate (3.27) is a direct consequence of (3.28),(3.33) and (3.36). *q.e.d.*

Proof of Theorem 3.1 Combining the estimates provided by Lemmas 3.1 - 3.4 and summing up over all $F \in \mathcal{M}^{(1)}$ readily gives (3.1). *q.e.d.*

4. Oscillation reduction. Besides the reliability (2.17) of the error estimator and the error reduction property (4.1), another important tool to establish the main convergence result is the following oscillation reduction:

Theorem 4.1. *There exist constants* $0 < \xi < 1$ *and* $C_2 > 0$ *, depending only on the data* χ, κ *, the constant* Θ_2 *in the bulk criterion* (2.12) *and on the shape regularity of the triangulations, such that*

$$osc_h^2 \ \leq \ \xi \ osc_H^2 \ + \ C_2 \ |||\mathbf{j_h} - \mathbf{j_H}|||^2 \ . \tag{4.1}$$

Proof. We set $\boldsymbol{\delta}_\mathbf{H} := \mathbf{j_h} - \mathbf{j_H}$. Then, for $T' \in \mathcal{T}_H$ and $T \in \mathcal{T}_h(T')$ we define $S_T^{(\nu)}(\boldsymbol{\delta}_\mathbf{H}), 1 \leq \nu \leq 2$, by means of

$$S_T^{(1)}(\boldsymbol{\delta}_\mathbf{H}) \ := \ \mathbf{curl}(\chi\mathbf{curl}(\boldsymbol{\delta}_\mathbf{H}) + \kappa\boldsymbol{\delta}_\mathbf{H} \quad , \quad S_T^{(2)}(\boldsymbol{\delta}_\mathbf{H}) \ := \ \mathrm{div}(\kappa\boldsymbol{\delta}_\mathbf{H}) \ . \tag{4.2}$$

In much the same way, for $F' \in \mathcal{F}_H(\Omega)$ and $F \in \mathcal{F}_h(F')$ we define $S_F^{(\nu)}(\boldsymbol{\delta}_\mathbf{H}), 1 \leq \nu \leq 2$, according to

$$S_F^{(1)}(\boldsymbol{\delta}_\mathbf{H}) \ := \ [\chi\mathbf{curl}(\boldsymbol{\delta}_\mathbf{H}) \wedge \mathbf{n}_F]_F \quad , \quad S_F^{(2)}(\boldsymbol{\delta}_\mathbf{H}) \ := \ [\mathbf{n}_F \cdot \kappa\boldsymbol{\delta}_\mathbf{H}]_F \ . \tag{4.3}$$

It follows readily from (4.2) and (4.3) that for $1 \leq \nu \leq 2$,

$$R_T^{(\nu)}(\mathbf{j_H}) \ := \ R_T^{(\nu)}(\mathbf{j_H}) - S_T^{(\nu)}(\boldsymbol{\delta}_\mathbf{h}) \quad , \quad R_F^{(\nu)}(\mathbf{j_H}) \ := \ R_F^{(\nu)}(\mathbf{j_H}) - S_F^{(\nu)}(\boldsymbol{\delta}_\mathbf{h}) \ . \tag{4.4}$$

We set

$$\overline{S}_T^{(\nu)}(\boldsymbol{\delta}_\mathbf{H}) \ := \ |T|^{-1} \int_T S_T^{(1)}(\boldsymbol{\delta}_\mathbf{H}) \ dx \quad , \quad \overline{S}_F^{(1)}(\boldsymbol{\delta}_\mathbf{H}) \ := \ |F|^{-1} \int_F S_F^{(1)}(\boldsymbol{\delta}_\mathbf{H}) \ d\sigma \ .$$

Observing (2.9) and (2.10), for $F \in \mathcal{F}_h(F'), \omega_F = T_+ \cup T_-, T_\pm \in \mathcal{T}_h$, Young's inequality implies that for some $\varepsilon > 0$

$$
\begin{aligned}
&(osc_{h,F}^{(1)})^2 \ \le \qquad\qquad (4.5)\\
&\le \ \frac{h_{T_+}^2}{m_+}\big((1+\varepsilon)\|R_{T_+}^{(1)}(\mathbf{j_H}) - \overline{R}_{T_+}^{(1)}(\mathbf{j_H})\|_{0,T_+}^2 \ + \ (1+\varepsilon^{-1})\|S_{T_+}^{(1)}(\boldsymbol{\delta}_\mathbf{H}) - \overline{S}_{T_+}^{(1)}(\boldsymbol{\delta}_\mathbf{H})\|_{0,T_+}^2\big) \ + \\
&+ \ \frac{h_{T_+}^2}{m_+}\big((1+\varepsilon)\|R_{T_+}^{(2)}(\mathbf{j_H}) - \overline{R}_{T_+}^{(2)}(\mathbf{j_H})\|_{0,T_+}^2 \ + \ (1+\varepsilon^{-1})\|S_{T_+}^{(2)}(\boldsymbol{\delta}_\mathbf{H}) - \overline{S}_{T_+}^{(2)}(\boldsymbol{\delta}_\mathbf{H})\|_{0,T_+}^2\big) \ + \\
&+ \ \frac{h_{T_-}^2}{m_-}\big((1+\varepsilon)\|R_{T_-}^{(1)}(\mathbf{j_H}) - \overline{R}_{T_-}^{(1)}(\mathbf{j_H})\|_{0,T_-}^2 \ + \ (1+\varepsilon^{-1})\|S_{T_-}^{(1)}(\boldsymbol{\delta}_\mathbf{H}) - \overline{S}_{T_-}^{(1)}(\boldsymbol{\delta}_\mathbf{H})\|_{0,T_-}^2\big) \ + \\
&+ \ \frac{h_{T_-}^2}{m_-}\big((1+\varepsilon)\|R_{T_-}^{(2)}(\mathbf{j_H}) - \overline{R}_{T_-}^{(2)}(\mathbf{j_H})\|_{0,T_-}^2 \ + \ (1+\varepsilon^{-1})\|S_{T_-}^{(2)}(\boldsymbol{\delta}_\mathbf{H}) - \overline{S}_{T_-}^{(2)}(\boldsymbol{\delta}_\mathbf{H})\|_{0,T_-}^2\big) \ , \\
&(osc_{h,F}^{(2)})^2 \ \le \qquad\qquad (4.6)\\
&\le \ h_F\big((1+\varepsilon)\|R_F^{(1)}(\mathbf{j_H}) - \overline{R}_F^{(1)}(\mathbf{j_H})\|_{0,F}^2 \ + \ (1+\varepsilon^{-1})\|S_F^{(1)}(\boldsymbol{\delta}_\mathbf{H}) - \overline{S}_F^{(1)}(\boldsymbol{\delta}_\mathbf{H})\|_{0,F}^2\big) \ + \\
&\quad + \ h_F\big((1+\varepsilon)\|R_F^{(2)}(\mathbf{j_H}) - \overline{R}_F^{(2)}(\mathbf{j_H})\|_{0,F}^2 \ + \ (1+\varepsilon^{-1})\|S_F^{(2)}(\boldsymbol{\delta}_\mathbf{H}) - \overline{S}_F^{(2)}(\boldsymbol{\delta}_\mathbf{H})\|_{0,F}^2\big) \ .
\end{aligned}
$$

Now, for $1 \le \nu \le 2$, we have

$$\|S_{T_\pm}^{(\nu)}(\boldsymbol{\delta}_\mathbf{H}) - \overline{S}_{T_\pm}^{(\nu)}(\boldsymbol{\delta}_\mathbf{H})\|_{0,T_\pm} \le \|S_{T_\pm}^{(\nu)}(\boldsymbol{\delta}_\mathbf{H})\|_{0,T_\pm} \ , \qquad (4.7)$$

$$\|S_F^{(\nu)}(\boldsymbol{\delta}_\mathbf{H}) - \overline{S}_F^{(\nu)}(\boldsymbol{\delta}_\mathbf{H})\|_{0,F} \le \|S_F^{(\nu)}(\boldsymbol{\delta}_\mathbf{H})\|_{0,F} \ . \qquad (4.8)$$

In order to obtain an upper bound for $\|S_{T_\pm}^{(\nu)}(\boldsymbol{\delta}_\mathbf{H})\|_{0,T_\pm}, 1 \le \nu \le 2$, in view of

$$\mathbf{curl}(\chi\mathbf{curl}(\boldsymbol{\delta}_\mathbf{H})) \ = \ \chi \ \mathbf{curl}(\mathbf{curl}(\boldsymbol{\delta}_\mathbf{H})) \ + \ \mathbf{grad}(\chi) \wedge \mathbf{curl}(\boldsymbol{\delta}_\mathbf{H})$$

and $\mathbf{curl}(\mathbf{curl}(\boldsymbol{\delta}_\mathbf{H})) = \mathbf{0}$ on $T \in \mathcal{T}_h$, we find

$$\|S_T^{(1)}(\boldsymbol{\delta}_\mathbf{H})\|_{0,T}^2 \ \le \ \max\big(\|\mathbf{grad}(\chi)\|_{\infty,T}, \|\kappa\|_{\infty,T}\big) \ \|\boldsymbol{\delta}_\mathbf{H}\|_{curl,T}^2 \ . \qquad (4.9)$$

Likewise, observing

$$\mathrm{div}(\kappa\boldsymbol{\delta}_\mathbf{H}) \ = \ \kappa \ \mathrm{div}(\boldsymbol{\delta}_\mathbf{H}) \ + \ \mathbf{grad}(\kappa) \cdot \boldsymbol{\delta}_\mathbf{H}$$

and $\mathrm{div}(\boldsymbol{\delta}_\mathbf{H}) = 0$ on $T \in \mathcal{T}_h$, we obtain

$$\|S_T^{(2)}(\boldsymbol{\delta}_\mathbf{H})\|_{0,T}^2 \ \le \ \|\mathbf{grad}(\kappa)\|_{\infty,T} \ \|\boldsymbol{\delta}_\mathbf{H}\|_{0,T}^2 \ . \qquad (4.10)$$

On the other hand, to derive an upper bound for $\|S_F^{(\nu)}(\boldsymbol{\delta}_{\mathbf{H}})\|_{0,F}, 1 \le \nu \le 2$, we have

$$\|S_F^{(1)}(\boldsymbol{\delta}_{\mathbf{H}})\|_{0,F}^2 \lesssim h_F^{-1} \|\chi \boldsymbol{\delta}_{\mathbf{H}}\|_{curl,\omega_F}^2 , \ \|S_F^{(2)}(\boldsymbol{\delta}_{\mathbf{H}})\|_{0,F}^2 \lesssim h_F^{-1} \|\kappa \boldsymbol{\delta}_{\mathbf{H}}\|_{div,\omega_F}^2 . \quad (4.11)$$

Hence, summarizing (4.9),(4.10) and (4.11), there exists a constant $C_D > 0$, depending on the data χ and κ, such that for $1 \le \nu \le 2$

$$h_{T_\pm}^2 \|S_{T_\pm}^{(\nu)}(\boldsymbol{\delta}_{\mathbf{H}})\|_{0,T_\pm}^2 \le C_D \, |||\boldsymbol{\delta}_{\mathbf{H}}|||^2 \quad , h_F \|S_F^{(\nu)}(\boldsymbol{\delta}_{\mathbf{H}})\|_{0,F}^2 \le C_D \, |||\boldsymbol{\delta}_{\mathbf{H}}|||^2 . \quad (4.12)$$

Moreover, due to the refinement strategy in MARK, for $F' \in \mathcal{F}_H(\Omega)$ such that $F' = T'_+ \cap T'_-, T'_\pm \in \mathcal{T}_H$, and $F \in \mathcal{F}_h(F'), F = T_+ \cap T_-, T_\pm \in \mathcal{T}_h(T'_\pm)$, we have

$$h_F \le \tau_{F'} \, h_{F'} \quad , \quad h_{T_\pm} \le \tau_{T'_\pm} \, h_{T'_\pm} , \quad (4.13)$$

where $\tau_{F'}, \tau_{T'_\pm} \le \tau_0$, if $F' \in \mathcal{M}^{(2)}$, and $\tau_{F'} = \tau_{T'_\pm} = 1$, otherwise.

Consequently, in view of (4.5),(4.6) and (4.12),(4.13) we obtain

$$\begin{aligned} osc_{h,F'}^2 &= \sum_{F \in \mathcal{F}_h(F')} osc_{h,F}^2 \le \quad (4.14) \\ &\le (1+\varepsilon) \max(\tau_{F'}, \tau_{T'_\pm}^2) \, osc_{H,F'}^2 + (1+\varepsilon^{-1}) \, C_D \, |||\boldsymbol{\delta}_{\mathbf{H}}|||_{\omega_{F'}}^2 . \end{aligned}$$

Summing up over all $F' \in \mathcal{F}_H(\Omega)$, the bulk criterion (2.12) yields

$$\begin{aligned} &\sum_{F' \in \mathcal{F}_H(\Omega)} \max(\tau_{F'}, \tau_{T'_\pm}^2) \, osc_{H,F'}^2 \le \\ &\le \tau_0 \sum_{F' \in \mathcal{M}^{(2)}} osc_{H,F'}^2 + \sum_{F' \in \mathcal{F}_H(\Omega) \setminus \mathcal{M}^{(2)}} osc_{H,F'}^2 \le (1 - (1-\tau_0)\Theta_2) \, osc_H^2 . \end{aligned}$$

Hence, by means of (4.14)

$$osc_h^2 \le (1+\varepsilon) \, (1-(1-\tau_0)\Theta_2) \, osc_H^2 + (1+\varepsilon^{-1}) \, \gamma \, C_D \, |||\boldsymbol{\delta}_{\mathbf{H}}|||^2 ,$$

where $\gamma > 0$ is a constant, depending only on the shape regularity of the triangulations, which accounts for the finite overlap of the $\omega_{F'}, F' \in \mathcal{F}_H(\Omega)$.

Finally, if we choose $\varepsilon < (1-\tau_0)\Theta_2/(1-(1-\tau_0)\Theta_2)$, the assertion follows with $\xi := (1+\varepsilon)(1-(1-\tau_0)\Theta_2)$ and $C_2 := (1+\varepsilon^{-1})\gamma C_D$. *q.e.d.*

5. Proof of Theorem 2.1. The reliability (2.17) and the error reduction (3.1) imply

$$|||\mathbf{j_h} - \mathbf{j_H}|||^2 \ \geq \ C_1^{-1} \ |||\mathbf{j} - \mathbf{j_H}|||^2 \ - \ osc_H^2 \ . \tag{5.1}$$

On the other hand, the orthogonality property $a(\mathbf{j} - \mathbf{j_h}, \mathbf{q_h}) \ = \ 0, \mathbf{q_h} \in \mathbf{Nd_{1,0}}(\Omega, \mathcal{T}_h)$ gives

$$|||\mathbf{j_h} - \mathbf{j_H}|||^2 \ = \ |||\mathbf{j} - \mathbf{j_H}|||^2 \ - \ |||\mathbf{j} - \mathbf{j_h}|||^2 \ ,$$

and hence, for some $0 < \varepsilon < 1$ we get

$$|||\mathbf{j} - \mathbf{j_h}|||^2 \ = \ |||\mathbf{j} - \mathbf{j_H}|||^2 \ - \ \varepsilon \ |||\mathbf{j_h} - \mathbf{j_H}|||^2 \ - \ (1-\varepsilon) \ |||\mathbf{j_h} - \mathbf{j_H}|||^2 \ . \tag{5.2}$$

Using (5.1) in (5.2) yields

$$|||\mathbf{j} - \mathbf{j_h}|||^2 \ \leq \ (1 - \varepsilon C_1^{-1}) \ |||\mathbf{j} - \mathbf{j_H}|||^2 + \varepsilon \ osc_H^2 - (1-\varepsilon) \ |||\mathbf{j_h} - \mathbf{j_H}|||^2 \ .$$

Incorporating the oscillation reduction property (4.1) results in

$$|||\mathbf{j} - \mathbf{j_h}|||^2 + C \ osc_h^2 \ \leq \ \rho_1 \ |||\mathbf{j} - \mathbf{j_H}|||^2 + (\varepsilon + (1-\varepsilon) C_2^{-1} \xi) \ osc_H^2 \ ,$$

where $\rho_1 := 1 - \varepsilon C_1^{-1} < 1$ and $C := (1-\varepsilon)C_2^{-1}$. If $0 < \rho_2 < 1$ is such that $\xi < \rho_2$ and if we choose ε according to

$$\varepsilon \ = \ \frac{C_2^{-1} \ (\rho_2 - \xi)}{1 + C_2^{-1} \ (\rho_2 - \xi)} \ ,$$

the assertion follows with $\rho := \max(\rho_1, \rho_2)$. *q.e.d.*

6. Numerical results. The performance of the adaptive scheme is illustrated by some representative numerical examples. The first one, Example 1, deals with an edge singularity caused by the L-shaped domain

$$\Omega \ := \ (-1,+1)^3 \setminus [0,1]^2 \times [-1,+1] \ .$$

The coefficients χ, κ are given by $\chi = \kappa = 1$ and the source term is chosen such that

$$\mathbf{j} \ = \ \mathbf{grad}(r^{2/3} \sin(\frac{2}{3}\phi)) \quad \text{(in cylindrical coordinates)} \ .$$

is the exact solution of the problem. Homogeneous Neumann boundary conditions are given on $\Gamma_N := \{0\}\times[0,1]\times[-1,+1]\cup[0,1]\times\{0\}\times[-1,+1]\cup\{x \in \overline{\Omega}|x_3 = \pm 1\}$, whereas inhomogeneous Dirichlet boundary conditions (according to the exact solution) are imposed elsewhere on Γ.

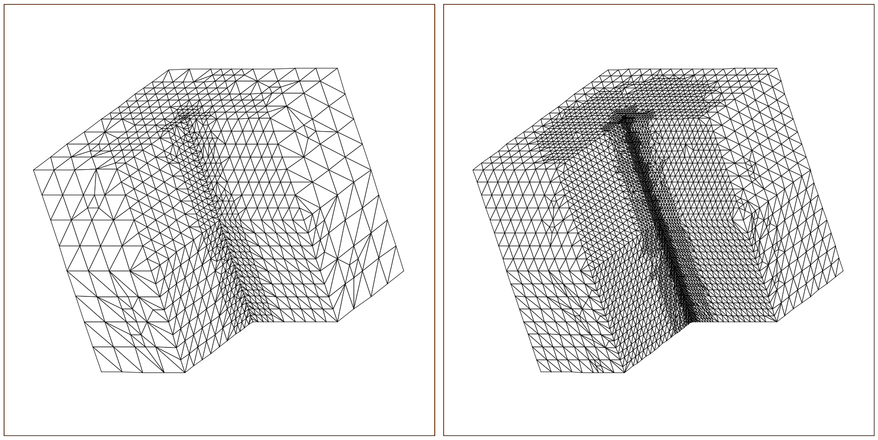

FIG. 6.1. *Example 1: Adaptively generated grid after 5 (left) and 7 (right) refinement steps ($\Theta_i = 0.4, 1 \leq i \leq 2$, in the bulk criteria)*

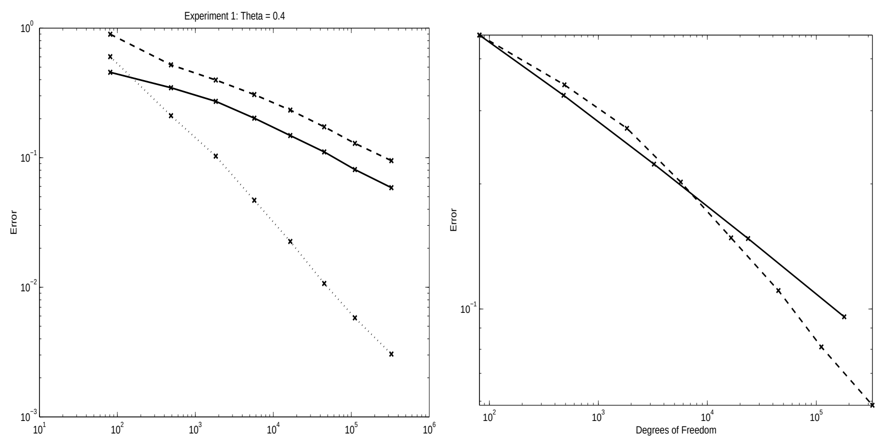

FIG. 6.2. *Example 1: True error (straight line), error estimator (dashed line) and data oscillations (dotted line) for $\Theta_i = 0.4, 1 \leq i \leq 2$ (left), adaptive refinement (straight line) versus uniform refinement (dashed line) (right)*

An initial triangulation with 81 degrees of freedom has been created by the grid generator NETGEN (cf. [29]). Figure 6.1 displays the adaptively refined grid after 5 (left) and 7 (right) refinement steps where the universal constants $\Theta_i, 1 \leq i \leq 2$,

Table 6.1

Example 1: True error $|||\mathbf{j} - \mathbf{j_H}|||$, error estimator $\boldsymbol{\eta}_\mathbf{H}$, oscillations $\mathbf{osc_H}$, and percentages of faces refined according to the bulk criteria ($\Theta_i = 0.4, 1 \leq i \leq 2$)

l	$\mathbf{N_{dof}}$	$|||\mathbf{j} - \mathbf{j_H}|||$	$\boldsymbol{\eta}_\mathbf{H}$	$\mathbf{osc_H}$	$\mathbf{M}\boldsymbol{\eta}$	$\mathbf{M_{osc}}$
0	81	4.56e-01	8.97e-01	6.02e-01	15.71	18.57
1	488	3.46e-01	5.20e-01	2.11e-01	6.48	4.97
2	1829	2.72e-01	3.98e-01	1.03e-01	4.30	4.94
3	5707	2.02e-01	3.07e-01	4.69e-02	4.18	2.87
4	16526	1.48e-01	2.33e-01	2.26e-02	3.94	4.50
5	44958	1.11e-01	1.73e-01	1.07e-02	4.04	4.13
6	11379	8.10e-02	1.29e-01	5.80e-03	4.37	4.87
7	327303	5.87e-02	9.49e-02	3.05e-03	3.95	1.72

in the bulk criteria (2.11),(2.12) have been chosen according to $\Theta_1 = \Theta_2 = 0.4$. We observe a pronounced refinement in a small vicinity of the edge singularity.

Figure 6.2 (left) shows the history of the refinement process in terms of the true error, the error estimator η_H and the oscillations osc_H, whereas Figure 6.2 (right) reflects the benefits of adaptive versus uniform refinement. More detailed information is given in Table 6.1. In particular, the last two columns contain the percentages $\mathbf{M}\boldsymbol{\eta}$ and $\mathbf{M_{osc}}$ of faces marked for refinement in the step MARK of the adaptive loop according to the bulk criterion (2.11) and (2.12), respectively.

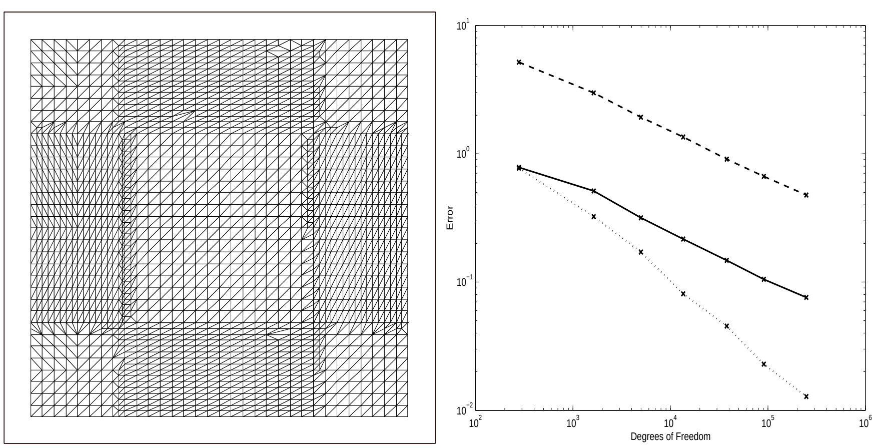

Fig. 6.3. *Example 2: Cross section ((x_1, x_2)-plane) of the adaptively generated grid (left) after 7 refinement steps ($\Theta_i = 0.4, 1 \leq i \leq 2$, in the bulk criteria) and history of the refinement process (right) [true error (straight line), error estimator (dashed line) and data oscillations (dotted line)]*

Example 2 illustrates the adaptive refinement process in case of discontinuous coefficients. The computational domain is $\Omega = (-1, +1)^3$ and the coefficients χ, κ are given by

$$\chi \ = \ 1 \ , \ \kappa \ = \ \begin{cases} 1 & , \quad \max(|x_1|,|x_2|,|x_3|) \le 1/2 \\ 0 & , \quad \text{elsewhere} \end{cases} \quad .$$

The right-hand side $\mathbf{f}$ and the boundary conditions have been chosen such that $\mathbf{j} = (0, 0, \sin(\pi x_1))$ is the exact solution. The initial grid with 279 degrees of freedom has been generated by NETGEN.

Figure 6.3 shows the (x_1, x_2)-cross section at $x_3 = 0$ of the adaptively refined grid after 6 refinement steps with a proper resolution of the material interface on the left and the history of the refinement process on the right. Again, more detailed information is provided in Table 6.2.

TABLE 6.2
Example 2: True error $|||\mathbf{j} - \mathbf{j_H}|||$, *error estimator* $\boldsymbol{\eta}_\mathbf{H}$, *oscillations* $\mathbf{osc_H}$, *and percentages of faces refined according to the bulk criteria* ($\Theta_i = 0.4, 1 \le i \le 2$)

l	N_{dof}	$\|\|\|\mathbf{j} - \mathbf{j_H}\|\|\|$	η_H	osc_H	$M\eta$	M_{osc}
0	**279**	**7.84e-01**	**5.18e+00**	**7.73e-01**	**8.89**	**15.93**
1	**1634**	**5.13e-01**	**2.99e+00**	**3.24e-01**	**8.32**	**6.02**
2	**4980**	**3.17e-01**	**1.93e+00**	**1.71e-01**	**5.75**	**4.51**
3	**13529**	**2.16e-01**	**1.35e+00**	**8.10e-02**	**7.74**	**5.79**
4	**37810**	**1.48e-01**	**9.08e-01**	**4.54e-02**	**8.49**	**4.36**
5	**90668**	**1.05e-01**	**6.67e-01**	**2.29e-02**	**8.71**	**2.54**
6	**247681**	**7.59e-02**	**4.77e-01**	**1.28e-02**	**6.71**	**4.14**

We expect a higher impact of the data oscillations on the adaptive refinement process in case of strongly varying coefficients. Therefore, Example 3 and Example 4 deal with the case of oscillating coefficients. The computational domain is $\Omega := (-1, +1)^3$, and $\chi = 1.5 + \sin(2\pi x_1)\sin(2\pi x_2)\sin(2\pi x_3), \kappa = 1$ in Example 2, whereas in Example 3 the roles of the coefficients are reversed, i.e., $\chi = 1, \kappa = 1.5 + \sin(2\pi x_1)\sin(2\pi x_2)\sin(2\pi x_3)$. In both examples, the right-hand side $\mathbf{f}$ and the boundary conditions have been chosen such that $\mathbf{j} = (0, 0, \sin(\pi x_1))$ is the exact solution. For both examples, a coarse initial grid has been created by using NETGEN resulting 19 degrees of freedom.

Figure 6.4 displays the history of the refinement process for Example 3 (left) resp. Example 4 (right), and Tables 6.3 and 6.4 provide detailed information including the percentages of faces marked for refinement. It can be clearly seen that at the beginning of the adaptive process the oscillation terms significantly contribute to the refinement, whereas at a later stage (when the data oscillations have been resolved) the process is dominated by the error estimator.

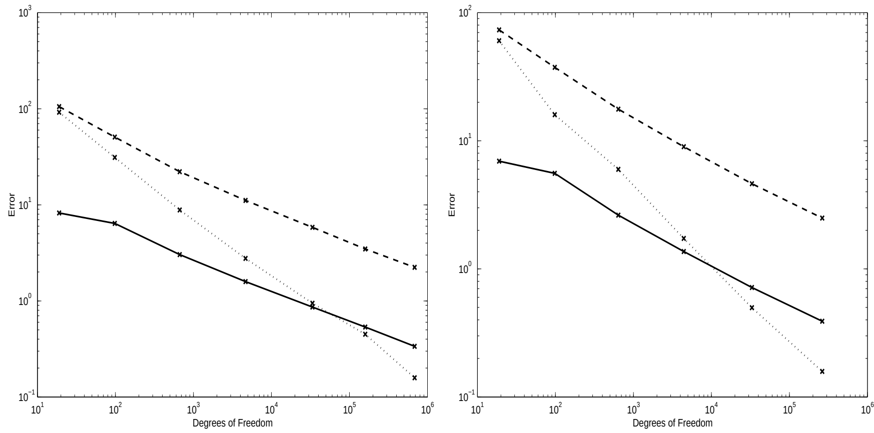

FIG. 6.4. *Examples 3 and 4: History of the refinement process for Example 3 (left) and Example 4 (right) ($\Theta_i = 0.6, 1 \leq i \leq 2$, in the bulk criteria) [true error (straight line), error estimator (dashed line) and data oscillations (dotted line)]*

TABLE 6.3
Example 3: True error $|||\mathbf{j} - \mathbf{j_H}|||$, error estimator $\boldsymbol{\eta}_\mathbf{H}$, oscillations $\mathbf{osc_H}$, and percentages of faces refined according to the bulk criteria ($\Theta_i = 0.6, 1 \leq i \leq 2$)

l	$\mathbf{N_{dof}}$	$\mathbf{\|\|\|j - j_H\|\|\|}$	$\boldsymbol{\eta}_\mathbf{H}$	$\mathbf{osc_H}$	$\mathbf{M}\boldsymbol{\eta}$	$\mathbf{M_{osc}}$
0	**19**	**8.23e+00**	**1.05e+02**	**9.20e+01**	**66.67**	**66.67**
1	**98**	**6.41e+00**	**5.08e+01**	**3.12e+01**	**48.61**	**50.00**
2	**667**	**3.03e+00**	**2.21e+01**	**8.85e+00**	**38.27**	**41.96**
3	**4651**	**1.59e+00**	**1.11e+01**	**2.77e+00**	**30.04**	**27.99**
4	**33561**	**8.63e-01**	**5.83e+00**	**9.45e-01**	**26.59**	**12.76**
5	**159482**	**5.35e-01**	**3.47e+00**	**4.50e-01**	**25.97**	**4.82**
6	**684546**	**3.37e-01**	**2.23e+00**	**1.58e-01**	**12.56**	**9.28**

TABLE 6.4
Example 4: True error $|||\mathbf{j} - \mathbf{j_H}|||$, error estimator $\boldsymbol{\eta}_\mathbf{H}$, oscillations $\mathbf{osc_H}$, and percentages of faces refined according to the bulk criteria ($\Theta_i = 0.6, 1 \leq i \leq 2$)

l	$\mathbf{N_{dof}}$	$\mathbf{\|\|\|j - j_H\|\|\|}$	$\boldsymbol{\eta}_\mathbf{H}$	$\mathbf{osc_H}$	$\mathbf{M}\boldsymbol{\eta}$	$\mathbf{M_{osc}}$
0	**279**	**6.94e+00**	**7.34e+01**	**6.04e+01**	**66.67**	**66.67**
1	**98**	**5.57e+00**	**3.75e+01**	**1.60e+01**	**50.00**	**51.39**
2	**640**	**2.63e+00**	**1.77e+01**	**5.98e+00**	**41.17**	**41.71**
3	**4424**	**1.37e+00**	**8.99e+00**	**1.73e+00**	**32.95**	**32.88**
4	**33010**	**7.16e-01**	**4.63e+00**	**4.98e-01**	**28.87**	**25.73**
5	**263283**	**3.90e-01**	**2.49e+00**	**1.58e-01**	**24.54**	**7.41**

Acknowledgements. The authors thank Werner Schabert for providing the numerical examples. The work of the first author was supported by the NSF under Grant

No. DMS-0411403 and Grant No. DMS-0511611. The third author acknowledges the support from the Austrian Science Foundation (FWF) under Grant No. Start Y-192.

REFERENCES

[1] M. Ainsworth and J.T. Oden , A Posteriori Error Estimation in Finite Element Analysis, Wiley, Chichester, 2000

[2] C. Amrouche, C. Bernardi, M. Dauge, and V. Girault, Vector potentials in three-dimensional non-smooth domains, Math. Meth. Appl. Sci. **21** (1998), 823–864

[3] D. Arnold, R. Falk, and R. Winther, Multigrid in H(div) and H(curl), Numer. Math. **85** (2000), 197–218

[4] I. Babuska and T. Strouboulis, The Finite Element Method and its Reliability, Clarendon Press, Oxford, 2001

[5] W. Bangerth and R. Rannacher, Adaptive Finite Element Methods for Differential Equations, Lectures in Mathematics, ETH-Zürich, Birkhäuser, Basel, 2003

[6] R. Beck, P. Deuflhard, R. Hiptmair, R.H.W. Hoppe, and B. Wohlmuth, Adaptive multilevel methods for edge element discretizations of Maxwell's equations. Surveys of Math. in Industry **8** (1999), 271–312 (

[7] R. Beck, R. Hiptmair, R.H.W. Hoppe, and B. Wohlmuth, Residual based a posteriori error estimators for eddy current computation. M^2AN Math. Modeling and Numer. Anal. **34** (2000), 159–182

[8] R. Beck, R. Hiptmair, and B. Wohlmuth, Hierarchical error estimator for eddy current computation. In: Proc. 2nd European Conf. on Advanced Numer. Meth. (ENUMATH99), Jyväskylä, Finland, July 26-30, 1999 (Neittaanmäki, P. et al.; eds.), pp. 111–120, World Scientific, Singapore, 2000

[9] P. Binev, W. Dahmen, and R. DeVore. Adaptive finite element methods with convergence rates, Numer. Math. **97** (2004), 219–268

[10] A. Bossavit, Electromagnétism, en vue de la modélisation, Springer, Berlin-Heidelberg-New York, 1993

[11] A. Buffa and Ph. Ciarlet Jr., On traces for functional spaces realted to Maxwell's equations. Part I: An integration by parts formula in Lipschitz polyhedra, Math. Meth. Appl. Sci **24** (2001), 9–30

[12] A. Buffa and Ph. Ciarlet Jr., On traces for functional spaces realted to Maxwell's equations. Part II: Hodge decompositions on the boundary of Lipschitz polyhedra and applications, Math. Meth. Appl. Sci **24** (2001), 31–48

[13] A. Buffa, M. Costabel, and D. Sheen, On traces for $\mathbf{H}(\mathbf{curl},\Omega)$ in Lipschitz domains, J. Math. Anal. Appl. **276** (2002), 845–867

[14] C. Carstensen, S. Funken, W. Hackbusch, R.H.W. Hoppe, and P. Monk (Eds.), Computational Electromagnetics, Proc. GAMM Workshop, Kiel, January 2001, Lecture Notes in Computational Science and Engineering, Vol. 28, Springer, Berlin-Heidelberg-New York, 2003

[15] C. Carstensen and R.H.W. Hoppe, Convergence analysis of an adaptive edge finite element method for the 2d eddy current equations, J. Numer. Math. **13** (2005), 19–32

[16] C. Carstensen and R.H.W. Hoppe, Error reduction and convergence for an adaptive mixed finite element method, Math. Comp. **75**, 1033-1042, 2006

[17] C. Carstensen and R.H.W. Hoppe, Convergence analysis of an adaptive nonconforming finite element method, Numer. Math. **103**, 251-266, 2006

[18] W. Dörfler, A convergent adaptive algorithm for Poisson's equation, SIAM J. Numer. Anal. **33** (1996), 1106–1124

[19] K. Eriksson, D. Estep, P. Hansbo, and C. Johnson, Computational Differential Equations, Cambridge University Press, Cambridge, 1995

[20] R. Hiptmair, Multigrid method for Maxwell's equations, SIAM J. Numer. Anal. **36** (1998), 204–225

[21] R. Hiptmair, Finite elements in computational electromagnetism, Acta Numerica **11** (2002), 237–339

[22] P. Houston, I. Perugia, and D. Schötzau, Energy norm a posteriori error estimation for mixed discontinuous Galerkin approximations of the Maxwell operator, Comput. Methods Appl. Mech. Engrg. **194** (2005), 499–510

[23] K. Mekchay and R. Nochetto, Convergence of adaptive finite element methods for general second

order linear elliptic PDE, SIAM J. Numer. Anal. **43** (2005), 1803–1827
[24] P. Monk, Finite Element Methods for Maxwell's equations, Clarendon Press, Oxford, 2003
[25] P. Morin, R.H. Nochetto, and K.G. Siebert, Data oscillation and convergence of adaptive FEM, SIAM J. Numer. Anal. **38** (2000), 466–488
[26] J.-C. Nédélec, Mixed finite element in $\mathbb{R}^3$, Numer. Math. **35**(1980), 315-341
[27] P. Neittaanmäki and S. Repin, Reliable methods for mathematical modelling. Error control and a posteriori estimates, Elsevier, New York, 2004
[28] S. Reitzinger, and J. Schöberl, Algebraic multigrid for edge elements, Numer. Lin. Alg. Appl. **9** (2002), 223–238
[29] J. Schöberl, NETGEN - An advancing front 2D/3D-mesh generator based on abstract rules, Comput. Visual. Sci. **1** (1997), 41–52
[30] J. Schöberl, A posteriori error estimates for Maxwell equations, Math. Comp. (in press)
[31] R. Stevenson, Optimality of a standard adaptive finite element method, Found. Comput. Math., DOI 10.1007/s 10208-005-0183-0, 2006.
[32] R. Verfürth, A Review of A Posteriori Estimation and Adaptive Mesh-Refinement Techniques, Wiley-Teubner, New York, Stuttgart, 1996